DOI:10.1021/jf901614y

JOURNAL OF AGRICULTURAL AND FOOD CHEMISTRY
ARTICLE

Oxidation of the Dihydrochalcone Aspalathin Leads to Dimerization

NICOLE KRAFCZYK,[†] THERES HEINRICH,[†] ANDREA PORZEL,[§] AND MARCUS A. GLOMB*[,†]

[†]Institute of Chemistry, Food Chemistry, Martin-Luther-University Halle-Wittenberg, Kurt-Mothes-Strasse 2, 06120 Halle, Germany, and [§]Leibniz Institute of Plant Biochemistry, Weinberg 3, 06120 Halle, Germany

Aspalathin and nothofagin are typical ingredients of unfermented rooibos (Krafczyk, N.; Glomb, M. A. *J. Agric. Food Chem.* **2008**, *56*, 3368). During oxidation these dihydrochalcones were degraded to higher molecular weight browning products under aerated and nonenzymatic conditions. In the early stages of browning reactions aspalathin formed two dimers. These two compounds were unequivocally established as atropisomers stemming from oxidative A to B ring coupling. Multilayer countercurrent chromatography (MLCCC) and preparative high-performance liquid chromatography (HPLC) were applied to obtain pure substances. The purity and identity of isolated dimers were confirmed by different NMR experiments, HPLC-DAD-MS, and HR-MS. In parallel to the formation of chromophores during the fermentation of black tea, the formation of aspalathin dimers implies an important mechanistic channel for the generation of color during the processing of rooibos.

KEYWORDS: Rooibos tea; reactions of dihydrochalcones; dimerization; nonenzymatic browning; NMR; HPLC-DAD-MS; HR-MS

INTRODUCTION

Aspalathin and nothofagin are dihydrochalcones contained predominantly in unfermented rooibos. During the fermentation process, they are degraded. At the same time, browning products of higher molecular weight are formed, which are responsible for the characteristic red color of fermented rooibos. This browning phenomenon was only mentioned in previous literature; detailed mechanisms, structures, or the involvement of enzymes were not yet characterized (*2*).

Flavonoids are modified through enzymatic or nonenzymatic reactions (*3*). A main mechanistic pathway is the oxidation of the 3′,4′-dihydroxy functions of the B-ring to the corresponding *o*-quinones. The enzymatic reaction channel is catalyzed by the enzyme polyphenol oxidase (PPO). The formation of *o*-quinones is the rate-limiting step for further reactions. *o*-Quinones are then able to react with other polyphenols, proteins, or polysaccharides (*4*, *5*). In addition, condensation and further oxidation steps result in the formation of brown molecules called melanins (*6*, *7*).

Catechins, as the typical ingredients of tea (*Camellia sinensis*) are significantly degraded during the fermentation process. Catechins, which also contribute significantly to the overall flavor and astringency of tea, constitute 16−30% in unfermented green tea and 3−10% in fully fermented black tea, expressed on a dry matter basis (*8*). In the manufacturing of black tea, the monomeric flavan-3-ols undergo PPO-dependent oxidative polymerization, which leads to the formation of bisflavanols, theaflavins, thearubigins, and other oligomers (*9*). Except for bisflavanols, all compounds are of red or red-brown color.

On the basis of established polyphenol reactions, this work investigates the importance of the dihydrochalcone aspalathin for the formation of colored structures arising during the processing of rooibos tea. Different incubations revealed the importance of this dihydrochalcone in comparison to other flavonoids found in rooibos and black teas (*1*).

MATERIALS AND METHODS

Chemicals. Chemicals of the highest quality available were obtained from Roth (Karlsruhe, Germany) unless otherwise indicated. Methanol was of HPLC grade from Merck (Darmstadt, Germany). (−)-Epicatechin was purchased from Fluka (Taufkirchen, Germany). Methanol (MeOH-d_4) was obtained from Deutero GmbH (Kastellaun, Germany).

Extraction of Rooibos Tea. Fermented and unfermented rooibos tea from the Bieduow Valley of South Africa was obtained from Ronnefeldt (Worpswede, Germany).

Screening Extraction. Three grams of fermented rooibos was extracted with 30 mL of acetone/water (7:3, v/v) at 5 °C for 24 h under argon atmosphere and decanted. Acetone was removed under reduced pressure. The residual H_2O phase was successively extracted with diethyl ether (10 mL) and ethyl acetate (10 mL).

Extraction for Isolation of Substances. A 100 g amount of unfermented (green) rooibos was extracted according to the same procedure as described above (1 L of acetone/water (7:3, v/v)). The volume was 2 × 200 mL for each solvent. From the individual extracts, solvents were removed under reduced pressure.

Analytical HPLC-DAD-MS. A Jasco (Gross-Umstadt, Germany) quaternary gradient unit PU 2080, with degasser DG 2080-54, autosampler AS 2055, column oven (Jasco Jetstream II), and multiwavelength

*Author to whom correspondence should be addressed (e-mail marcus.glomb@chemie.uni-halle.de, fax ++49-345-5527341).

 Published on Web 07/14/2009

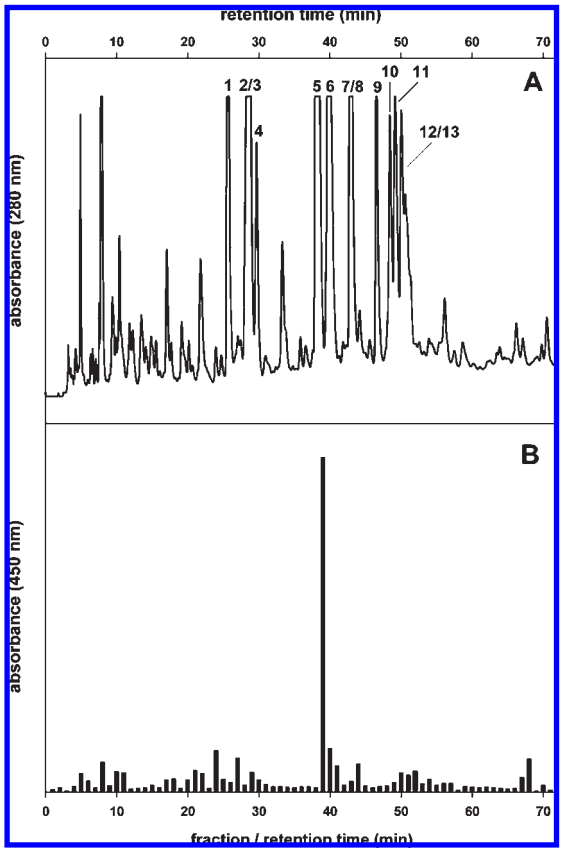

Figure 1. (**A**) HPLC-DAD chromatogram (method A) of ethyl acetate extract from fermented rooibos at λ = 280 nm. Peaks: 1, (*S*)-eriodictyol-6-*C*-β-D-glucopyranoside (26.3 min); 2, (*S*)-eriodictyol-8-*C*-β-D-glucopyranoside (29.1 min); 3, (*R*)-eriodictyol-6-*C*-β-D-glucopyranoside (29.5 min); 4, (*R*)-eriodictyol-8-*C*-β-D-glucopyranoside (30.4 min); 5, aspalathin (39.4 min); 6, orientin (40.9 min); 7/8, isoorientin/vitexin (44.1 min); 9, nothofagin (47.8 min); 10, isovitexin (49.7 min); 11, rutin (50.6 min); 12, hyperoside (51.6 min); 13, isoquercitrin (52.1 min). Retention times are given in parentheses. (**B**) Absorbance at λ = 450 nm of collected fractions after re-incubation.

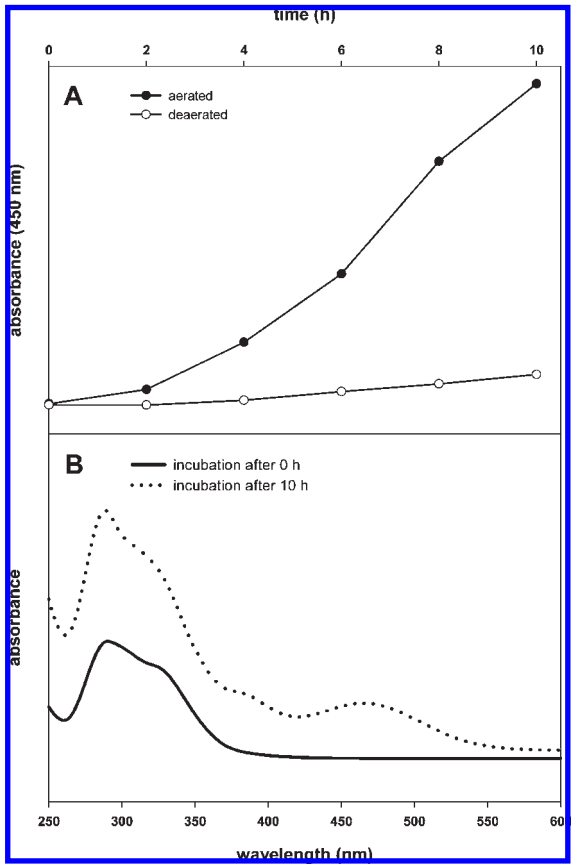

Figure 2. (**A**) Browning of aspalathin incubated under aerated and deaerated conditions. (**B**) Wavelength scan of aerated incubation after 0 and 10 h.

detector MD 2015 coupled to an Advantec fraction collector CHF122SB (Tokyo, Japan) was used. Alternatively, the detector was coupled to an API 4000 triple-quadruple mass spectrometer (Applied Biosystems, Foster City, CA). Chromatographic separations were performed on stainless steel columns (Vydac CRT 218TP54, 250 × 4.0 mm, RP 18, 5 μm, Hesperia, CA) using a flow rate of 1.0 mL min^{-1}. The mobile phase used was water (solvent A) and MeOH/water (7:3, v/v, solvent B). To both solvents (A and B) was added 0.6 mL L^{-1} heptafluorobutyric acid (HFBA). In *method A*, samples were injected at 10% B, and the gradient was then changed to 30% B in 30 min, to 65% B in 40 min, to 100% B in 2 min, and held at 100% B for 8 min. In *method B*, samples were injected at 10% B, and the gradient was then changed to 30% B in 30 min, to 52% B in 25 min, to 100% B in 2 min, and held at 100% B for 8 min. The column temperature was 25 °C. The effluent was monitored at 280 and 350 nm. For browning incubations, 100 fractions of 1 mL were collected in 100 min.

MS ionization of the analytes was achieved using the Turbospray ionization source operated in positive ions mode. The Turbospray settings were as follows: curtain gas (N_2) at 40 psi; ion source gases 1 and 2 both at 60 psi; source temperature at 550 °C; ion spray voltage at 4000 V; and collision gas pressure at 5 psi. Mass spectral data on precursor and product ions were collected. Declustering potential, entrance potential, collision energy, and cell exit potential were optimized for each analyte.

Incubation of Fractions. Fractions with eluted material from analytical HPLC-DAD were collected and evaporated. Then, fractions were dissolved in phosphate buffer (0.2 M, pH 7.4) and incubated (37 °C) for 48 h in a shaker incubator (New Brunswick Scientific, New Brunswick, NJ). The absorbance of these solutions was measured at 450 nm with a Jasco V-530 UV−vis spectrometer (Gross-Umstadt, Germany).

Incubation of Flavonoids. Isolated substances (4.5 mM) were dissolved in phosphate buffer (0.2 M, pH 7.4) and incubated (37 °C) for 8 h (24 h for aspalathin) in a shaker incubator (New Brunswick Scientific). After evaporation, the final residue was separated by HPLC-DAD.

Multilayer Countercurrent Chromatography (MLCCC). The MLCCC system (Ito, Multilayer Separator-Extractor model, P. C. Inc., Potomac, MD) was equipped with a Waters constant-flow pump (model 6000 A), a Zeiss spectrophotometer PM2D operating at 280 nm, and a sample injection valve with a 10 mL sample loop. Eluted liquids were collected in fractions of 16 mL with a fraction collector (LKB Ultrorac 7000). Chromatograms were recorded on a plotter (Servogor 200). The multilayer coil was prepared from 1.6 mm i.d. poly(tetrafluoroethylene) (PTFE) tubing. The total capacity was 240 mL. The MLCCC was run at a revolution speed of 800 rpm and a flow rate of 2 mL min^{-1} in head to tail mode.

For preparative isolation of dimers, aspalathin (22 mM) was dissolved in phosphate buffer (0.2 M, pH 7.4) and incubated (37 °C) for 4 h in a shaker incubator. The reactions were stopped by adding hydrochloric acid (1 N). Incubated samples were dissolved in the heavy phase and injected into the system. The solvent system for separation consisted of ethyl acetate/*n*-butanol/water (3:1:4 (v/v)).

Preparative HPLC-UV. A Besta HD 2-200 pump (Wilhelmsfeld, Germany) was used at a flow rate of 8 mL min^{-1}. Elution of materials was monitored by a UV detector (Jasco UV- 2075). Chromatographic separations were performed on stainless steel columns (Vydac CRT. 218TP1022, 250 × 23 mm, RP18, 10 μm). The mobile phase used was solvent A and B identical to the analytical HPLC-DAD system. From the individual chromatographic fractions solvents were removed under reduced pressure. After the addition of water, solutions of polyphenols were freeze-dried.

Accurate Mass Determination. The high-resolution positive and negative ion ESI mass spectra (HR-MS) were obtained from a Bruker

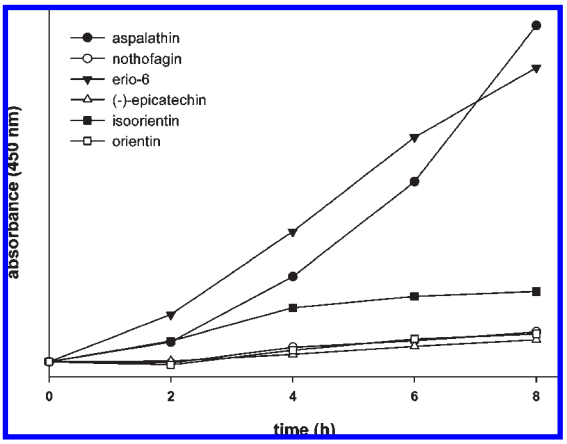

Figure 3. Incubations of aspalathin **5**, nothofagin **9**, (*S*)-eriodictyol-6-*C*-*β*-D-glucopyranoside **1** (erio-6), (−)-epicatechin, isoorientin **7**, and orientin **6** for 8 h. Formation of browning products was observed at λ = 450 nm.

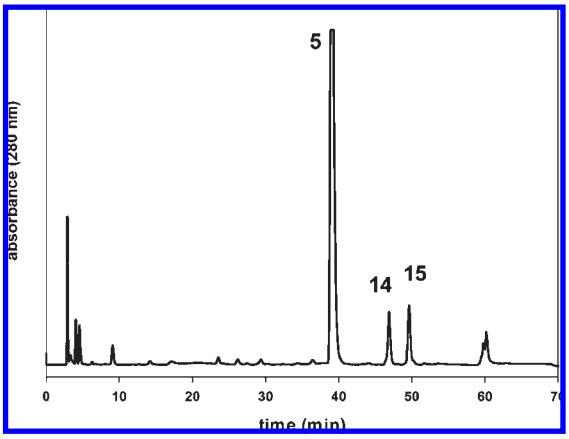

Figure 4. HPLC-DAD chromatograms (method B) of aspalathin **5** after an incubation time of 8 h (λ = 280 nm): aspalathin **5** (39.4 min, λ = 280 nm); dimer **14** (46.3 min, λ_{max} = 285 nm); dimer **15** (49.0 min, λ_{max} = 285 nm). Retention times and absorbance maxima are given in parentheses.

Apex III Fourier transform ion cyclotron resonance (FT-ICR) mass spectrometer (Bruker Daltonics, Billerica, MA) equipped with an Infinity cell, a 7.0 T superconducting magnet (Bruker, Karlsruhe, Germany), an RF-only hexapole ion guide, and an external electrospray ion source (Apollo; Agilent, off-axis spray). Nitrogen was used as drying gas at 150 °C. The samples were dissolved in methanol, and the solutions were introduced continuously via a syringe pump at a flow rate of 120 μL h^{-1}. The data were acquired with 256K data points and zero filled to 1024K by averaging 32 scans.

Nuclear Magnetic Resonance (NMR) Spectroscopy. NMR spectra were recorded on a Varian VNMRS 600 instrument (Palo Alto, CA). Chemical shifts are given relative to Me_4Si and were referenced to internal Me_4Si (δ = 0 ppm, ^{1}H) and internal CD_3OD (δ = 49.0 ppm, ^{13}C).

Circular Dichroism (CD) Spectroscopy. CD measurements were obtained on a Jasco J-815 CD spectrometer (Tokyo, Japan). The CD spectra were recorded from 195 to 400 nm in cells with a 0.1 cm path length. The following parameters were used: 0.5 s response, 50 nm min^{-1} scanning speed, 0.2 nm data acquisition interval, 10 accumulations, 1 nm bandwidth. CD samples were prepared by dissolving compounds **14** and **15** in methanol, leading to concentrations of 0.0643 mM for **14** and of 0.2571 mM for **15**, respectively. Measurements were made at 20 °C. Ellipticity was reported as mean molar ellipticity [θ] (deg cm^2 dmol^{-1}).

Transformation Experiments. Compound **14** was dissolved in water and heated in stages from 30 to 90 °C. The solvent was removed under reduced pressure. Then, material was analyzed by NMR and HPLC-DAD.

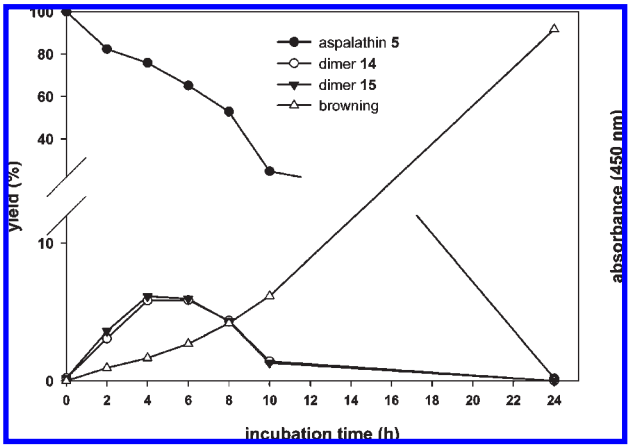

Figure 5. Incubation of aspalathin **5** leads to dimers **14** and **15** and browning (monitored at λ = 450 nm).

RESULTS AND DISCUSSION

During the fermentation process of rooibos, the color of the tea changes from dark green to red-brown. The compounds involved in these browning reactions were searched out by the following method: First, an absorbance maximum at about 450 nm was located for an aqueous infusion of fermented rooibos tea. Then, the ethyl acetate extract (screening extraction procedure) was separated by analytical HPLC-DAD, and eluted material was collected in 1 mL fractions. After re-incubation in phosphate buffer, the absorbance of each fraction was measured at 450 nm. Fermented rooibos was chosen in contrast to green rooibos, as it contains the widest variety of potential compounds, native and fermentation degradation products. **Figure 1** presents the HPLC-DAD chromatogram of ethyl acetate extract with the corresponding absorbances of re-incubated material. Aspalathin **5** was unequivocally established as the single most important player within the reaction to browning products. However, some other fractions responded to a minor extent and implied that browning is not exclusively related to the structure of aspalathin **5**. As we recently reported, oxidation of aspalathin **5** delivered several compounds characteristic for fermented rooibos: eriodictyol-*C*-*β*-D-glycopyranosides **1**−**4**, isoorientin **7** and orientin **6** (*1*). These degradation compounds have an absorbance maximum of 280 nm (**1**−**4**) and of 350 nm (**6** + **7**), respectively. To study the influence of oxidative mechanisms on the browning, isolated aspalathin **5** (*1*) was incubated under aerated and deaerated conditions during a period of 10 h. As depicted in **Figure 2** there was a change in absorbance maximum from 280 to 450 nm in the presence of oxygen. The behavior of this dihydrochalcone clearly suggests that the browning reaction is an oxygen-dependent process. Thus, not only the follow-up products orientin **6**, isoorientin **7**, (*S*)-eriodictyol-6-*C*-*β*-D-glucopyranoside **1** but also nothofagin **9** and (−)-epicatechin were incubated under aerated conditions (**Figure 3**). (−)-Epicatechin, a typical compound of green tea, showed only negligible browning reactions during the incubation process. The degradation of (−)-epicatechin during the fermentation of *C. sinensis* is based on the presence of enzymes (PPO). Thus, browning reactions of *C. sinensis* proceed completely differently in comparison to *Aspalathus linearis*. Nothofagin **9** consists of the same dihydrochalcone structure as aspalathin with the loss of one hydroxyl group and, thus, the *o*-dihydroxy function at the B-ring. Therefore, oxidation proceeds much more slowly, resulting in significantly reduced browning (**Figure 3**). The flavone-*C*-glycosides orientin **6** and isoorientin **7** also showed comparably slow degradation. Obviously, in addition to the o-hydroquinone moiety at the B-ring, the configuration of the

Table 1. ^{1}H (600 MHz) and ^{13}C NMR (125 MHz) Spectroscopic Data of Dimers **14** and **15** (in CD_3OD)[a,b] and Selected HMBC Correlations Observed for Both Dimers

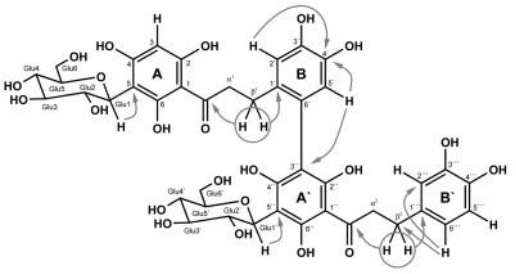

	dimer 14		dimer 15	
C/H	δ ^{1}H [ppm]	δ ^{13}C [ppm]	δ ^{1}H [ppm]	δ ^{13}C [ppm]
1	-	105,76[c]	-	105,74
2	-	163,94	-	163,99
3	5,882 (s, 1H)	95,91	5,880 (s, 1H)	95,87
4	-	164,86	-	164,85
5	-	104,13[d]	-	104,12[e]
6	-	165,71	-	165,72
CO^{1}	-	207,04	-	207,07
α^{1}	3,191 (m, 2 H)	46,14	3,144 (ddd, 1H, ^{2}J = 16,4 Hz, ^{3}J = 9,2 Hz, ^{3}J = 6,1 Hz) 3,226 (ddd, 1H, ^{2}J = 16,4 Hz, ^{3}J = 9,2 Hz, ^{3}J = 6,1 Hz)	46,09
β^{1}	2,605 (ddd, 1H, ^{2}J = 14,2 Hz, ^{3}J = 8,4 Hz, ^{3}J = 6,9 Hz) 2,693 (ddd, 1H, ^{2}J = 14,2 Hz, ^{3}J = 8,4 Hz, ^{3}J = 6,9 Hz)	29,16	2,600 (ddd, 1H, ^{2}J = 14,1 Hz, ^{3}J = 9,2 Hz, ^{3}J = 6,1 Hz) 2,680 (ddd, 1H, ^{2}J = 14,1 Hz, ^{3}J = 9,2 Hz, ^{3}J = 6,1 Hz)	29,14
1′	-	135,70	-	135,60
2′	6,806 (s, 1H)	117,74	6,804 (s, 1H)	117,82
3′	-	146,69	-	146,68
4′	-	144,88	-	144,87
5′	6,548 (s, 1H)	120,07	6,538 (s, 1H)	120,21
6′	-	122,77	-	122,73
Glu1	4,797 (d, 1H, ^{3}J = 9,9 Hz)	76,00	4,794 (d, 1H, ^{3}J = 9,9 Hz)	76,00
Glu2	3,933 (dd, 1H, ^{3}J = 9,9 Hz, ^{3}J = 8,7 Hz)	73,15	3,940 (dd, 1H, ^{3}J = 9,9 Hz, ^{3}J = 8,8 Hz)	73,14
Glu3	3,43 (m, 1H)	80,0	3,42 (m, 1H)	80,0
Glu4	3,45 (m, 1H)	71,5	3,43 (m, 1H)	71,5
Glu5	3,357 (ddd, 1H, ^{3}J = 9,5 Hz, ^{3}J = 5,0 Hz, ^{3}J = 2,2 Hz)	82,50	3,347 (ddd, 1H, ^{3}J = 9,2 Hz, ^{3}J = 5,1 Hz, ^{3}J = 2,4 Hz	82,50
Glu6	3,731 (dd, 1H, ^{2}J = 12,3 Hz, ^{3}J = 5,0 Hz) 3,83 (dd, 1H, ^{2}J = 12,3 Hz, ^{3}J = 2,2 Hz)	62,53	3,722 (dd, 1H, ^{2}J = 12,2 Hz, ^{3}J = 5,1 Hz) 3,819 (dd, 1H, ^{2}J = 12,2 Hz, ^{3}J = 2,4 Hz)	62,56
1″	-	105,46[c]	-	105,45
2″	-	161,32	-	161,28
3″	-	109,54	-	109,56
4″	-	161,47	-	161,49
5″	-	104,16[d]	-	104,13[e]
6″	-	163,06	-	163,09
CO^{2}	-	207,24	-	207,26
α^{2}	3,31 (m, 2H)[f]	47,7	3,31 (m, 2H)[f]	47,70
β^{2}	2,799 (t, 2H, ^{3}J = 7,7 Hz)	31,56	2,794 (t, 2H, ^{3}J = 7,7 Hz)	31,56
1‴	-	134,74	-	134,74
2‴	6,650 (d, 1H, ^{4}J = 2,0 Hz)	116,64	6,646 (d, 1H, ^{4}J = 2,0 Hz)	116,63
3‴	-	146,02	-	146,02
4‴	-	144,26	-	144,26
5‴	6,627 (d, 1H, ^{3}J = 8,1 Hz)	116,30	6,625 (d, 1H, ^{3}J = 8,0 Hz)	116,30
6‴	6,518 (dd, 1H, ^{3}J = 8,1 Hz, ^{4}J = 2,0 Hz)	120,71	6,511 (dd, 1H, ^{3}J = 8,0 Hz, ^{4}J = 2,0 Hz)	20,71
Glu1′	4,962 (d, 1H, ^{3}J = 9,9 Hz)	76,91	4,962 (d, 1H, ^{3}J = 9,9 Hz)	77,00
Glu2′	3,753 (dd, 1H, ^{3}J = 9,9 Hz, ^{3}J = 9,1 Hz)	74,13	3,756 (dd, 1H, ^{3}J = 9,9 Hz, ^{3}J = 9,1 Hz)	74,13
Glu3′	3,49 (m, 1H)	79,6	3,48 (m, 1H)	79,5
Glu4′	3,49 (m, 1H)	71,2	3,48 (m, 1H)	71,3
Glu5′	3,44 (m, 1H)	82,6	3,43 (m, 1H)	82,7
Glu6′	3,770 (dd, 1H, ^{2}J = 12,2 Hz, ^{3}J = 4,7 Hz) 3,88 (dd, 1H, ^{2}J = 12,2 Hz, ^{3}J = 2,3 Hz)	62,06	3,776 (dd, 1H, ^{2}J = 12,2 Hz, ^{3}J = 4,8 Hz) 3,876 (dd, 1H, ^{2}J = 12,2 Hz, ^{3}J = 2,2 Hz)	62,21

[a] δ, chemical shift; *J*, coupling constant. Hydrogen/carbon assignments were verified by HMBC, HMQC, and ^{13}C-DEPT measurements. [b] Chemical shifts with three (^{1}H) or two (^{13}C) positions after decimal point were taken from 1D NMR experiments; chemical shifts with two (^{1}H) or one (^{13}C) position after decimal point were taken from 2D NMR experiments. [c,d,e] Assignments may be interchanged. [f] The signal was overlapped with the solvent signal.

C-ring is of major importance to oxidation and thereby browning of flavonoids. This aspect was supported by the behavior of (*S*)-eriodictyol-6-*C*-β-D-glycopyranoside **1**, which showed a result similar to that of aspalathin **5**. As published earlier by us, the 6- and 8-*C*-β-eriodictyol monomers are directly related to the o-quinone of oxidized aspalathin **5**. Thus, the degradation of this dihydrochalcone was studied in more detail.

Figure 4 presents the HPLC-DAD chromatograms of an aerated aspalathin incubation at 8 and 48 h. Two distinct additional peaks emerged (**14**, **15**), but were completely degraded later to give uncharacteristic signals for colored material. The LC-ESI-MS-spectrum of **14** was identical to that of **15**. The structures delivered a pseudomolecular ion of *m*/*z* 925.4 [M + Na^+] and suggested dimerization of aspalathin **5**. This was confirmed by high-resolution mass spectrometry (**14**, *m*/*z* 925.23736 [M + Na^+] found; **15**, *m*/*z* 925.23802 [M + Na^+] found, *m*/*z* 925.23729 [M + Na^+] calcd for $C_{42}H_{46}O_{22}Na$). **Figure 5** shows the yields of **5**, **14**, and **15** during incubation in relation to increase of browning. Maximum concentration of dimers was reached after 4 h in the ratio 47:53 for dimer **14**/**15**. After 48 h, all compounds were completely degraded to brown end products, which gave the characteristic absorbance maximum at 450 nm.

On the basis of known flavonoid chemistry, oxidation-induced dimerization could be realized by (i) B → B′ ring, (ii) B → A′ ring,

and (iii) quinine methide → B′/A′ ring bonding. To identify and verify the structure of the dimers, aspalathin **5** was incubated for 4 h and dimers were isolated by MLCCC and preparative HPLC. Complete structure elucidation of authentic compounds was achieved by both 1D and 2D homonuclear ^{1}H and heteronuclear ^{1}H ^{13}C experiments. ^{1}H and ^{13}C NMR data of both substances and chemical shift assignments are provided in **Table 1**. NMR data unequivocally established the formation of dimers. Selected HMBC correlations are also shown in **Table 1**.

The proton signals of a three-spin system (B′-ring) and the singlet of an aromatic proton (A-ring) resemble in chemical shift and multiplet pattern those of aspalathin **5** (*1*). Only two further aromatic ^{1}H signals H-2′ (compound **14**, δ 6.806; compound **15**, δ 6.804), and H-5′ (compound **14**, δ 6.548; compound **15**, δ 6.538) appear, belonging to the B-ring due to their mutual HMBC correlations to C-1′, C-3′, and C-4′. The presence of the ^{3}J HMBC correlation between H-5′ and C-3′ proved unequivocally the proposed dimeric structures. Thus, the two aspalathin moieties are connected via a biaryl bond between C-6′ of the B-ring of one molecule and C-3′ of the A′-ring of a second molecule.

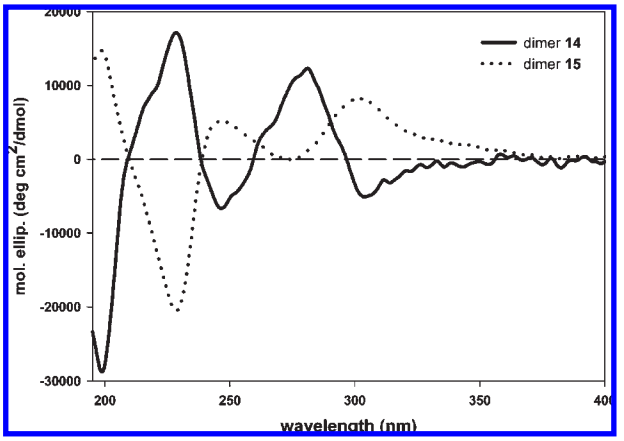

Figure 6. Circular dichroism spectra of dimers **14** and **15**.

In further support, HPLC-MS^2 experiments verified a loss of 452 mass units corresponding to one aspalathin molecule, which is expected for a dimeric structure. MS^2 experiments also evidenced the proposed structure by a loss of the B′-ring with α- and β-positions (*m*/*z* 137) and the loss of the A-ring with a glucose moiety (*m*/*z* 288). Fragment *m*/*z* 579 corresponded to the loss of two glucose moieties (324 mass units). Typical fragmentation patterns for glycosyl flavonoids $[M + H - 90]^+$, $[M + H - 120]^+$, and $[M + H - 150]^+$ were recorded, which were in line with Kazuno et al. (*10*).

With regard to all results, the structures of compounds **14** and **15** should be atropisomers. Indeed, CD measurements showed opposite Cotton effects (**Figure 6**). Due to the three substituents in the ortho-position to the biaryl axis C-6′C-3′ and the voluminous glucose moiety, free rotation is obviously restricted. Isomerization experiments conducted at elevated temperature showed that isolated **14** can be transformed into **15** to the same equilibrium (47:53 for **14**:**15**) found during oxidative degradation of aspalathin **5**.

Figure 7 depicts a plausible mechanism for the formation of aspalathin dimers based on oxidative coupling. This mechanism also plays an important role within enzymatic browning reactions of black tea (*C. sinensis*) for the formation of bisflavanols. These are key intermediates for the formation of colored structures as theaflavins and thearubigins (*11*). Thus, the elucidation of dimers during oxidative degradation of aspalathin suggests a major step forward to the understanding of browning mechanisms in rooibos. In addition, the kinetic data on aspalathin degradation imply

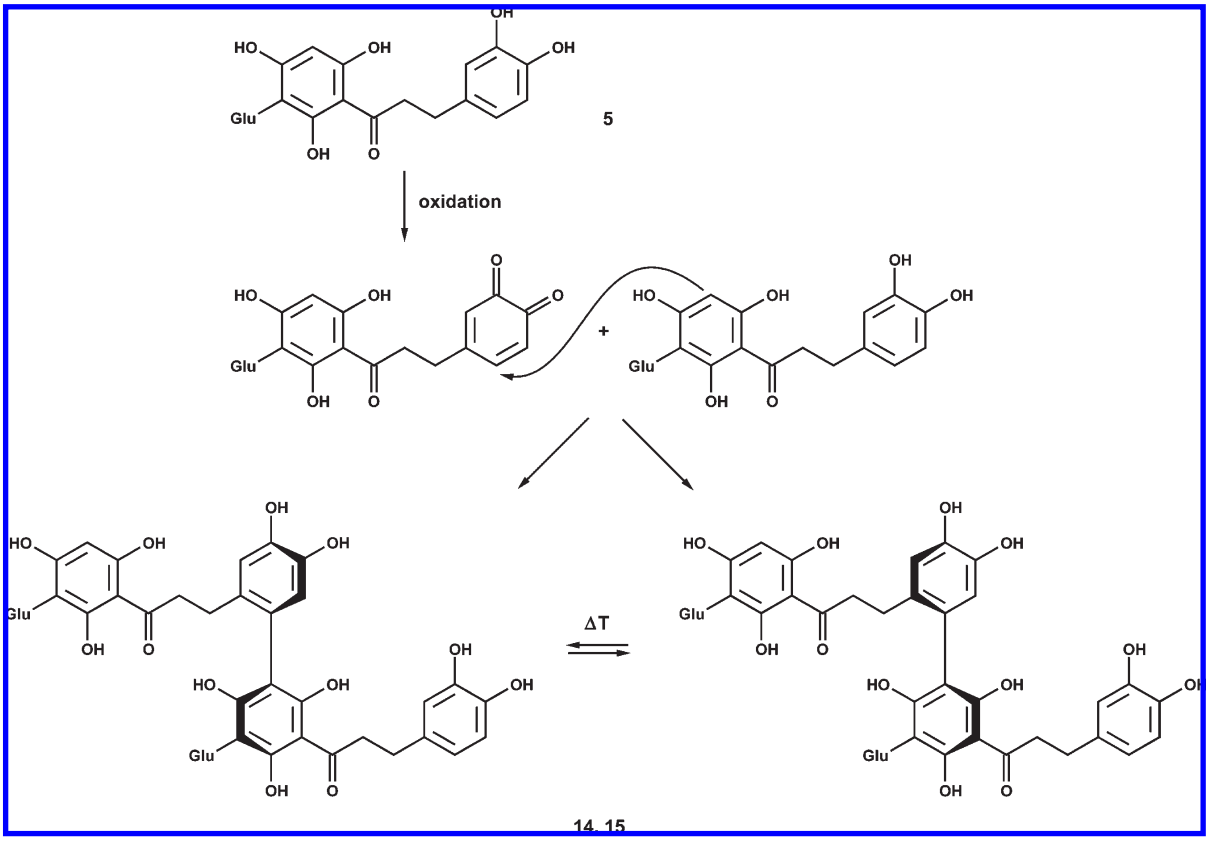

Figure 7. Dimers **14** and **15** are formed from aspalathin **5** by oxidative coupling. Glu = glucose.

that the formation of color during fermentation of rooibos (*A. linearis*) is mainly if not solely based on nonenzymatic mechanisms, in contrast to the processing of black tea (*C. sinensis*).

ACKNOWLEDGMENT

We thank J. Schmidt from the Leibniz Institute of Plant Biochemistry, Halle (Germany), for performing LC-MS/ accurate mass analysis.

LITERATURE CITED

(1) Krafczyk, N.; Glomb, M. A. Characterization of phenolic compounds in rooibos tea. *J. Agric. Food Chem.* **2008**, *56*, 3368–3376.
(2) Joubert, E. HPLC quantification of the dihydrochalcones, aspalathin and nothofagin in rooibos tea (*Aspalathus linearis*) as affected by processing. *Food Chem.* **1996**, *55*, 403–411.
(3) Spanos, G. A.; Wrolstad, R. E. Phenolics of apple, pear, and white grapes juices and their changes with processing and storage—a review. *J. Agric. Food Chem.* **1992**, *40*, 1478–1487.
(4) Li, Y.; Tanaka, T.; Kouno, I. Oxidative coupling of the pyrrogallol B-ring with a galloyl group during enzymatic oxidation of epigallocatechin 3-*O*-gallate. *Phytochemistry* **2007**, *68*, 1081–1088.
(5) Rohn, S.; Rawel, H. M.; Kroll, J. Antioxidant activity of protein-bound quercitin. *J. Agric. Food Chem.* **2004**, *52*, 4725–4729.
(6) Weeks, W. W.; Campos, M. P.; Moldoveanu, S. Biochemical and model chemical reactions for the basis of red pigment in flue-curred tobacco. *J. Agric. Food Chem.* **1993**, *41*, 1321–1328.
(7) Amiot, M. J.; Forget-Richard, F.; Goupy, P. Polyphenols, oxidation and color: progress in the chemistry of enzymatic and non-enzymatic derived products. *Herba Pol.* **1996**, *42*, 237–242.
(8) Khokhar, S.; Magnusdottir, S. G. M. Total phenol, catechin, and caffeine contents of teas commonly consumed in the United Kingdom. *J. Agric. Food Chem.* **2002**, *50*, 565–570.
(9) Harold, N.; Graham, P. D. Green tea composition, consumption, and polyphenol chemistry. *Prev. Med.* **1992**, *21*, 334–350.
(10) Kazuno, S.; Yanagida, M.; Shindo, N.; Murayama, K. Mass spectrometric identification and quantification of glycosyl flavonoids, including dihydrochalcones with neutral loss scan mode. *Anal. Biochem.* **2005**, *347*, 182–192.
(11) Tanaka, T.; Mine, C.; Inoue, K.; Matsuda, M.; Kouno, I. Synthesis of theaflavin from epicatechin and epigallocatechin by plant homogenates and role of epicatechin quinone in the synthesis and degradation of theaflavin. *J. Agric. Food Chem.* **2002**, *50*, 2142–2148.

Received May 14, 2009. Revised manuscript received July 3, 2009. Accepted July 04, 2009.